Electronic Supplementary Information on

Water Structure and Dynamics in the Hydration Layer of a Type III Anti-Freeze Protein

Z. Faidon Brotzakis,[a‡] Ilja K. Voets, [b], Huib J. Bakker [c], and Peter G. Bolhuis [*a]

[a] Van 't Hoff Institute for Molecular Sciences, Universiteit van Amsterdam, Science Park 904, 1098 XH Amsterdam, The Netherlands
[b] Laboratory of Macromolecular and Organic Chemistry, Laboratory of Physical Chemistry, and Institute for Complex Molecular Systems, Eindhoven University of Technology, Post Office Box 513, 5600 MB, Eindhoven, Netherlands.
[b] FOM Institute AMOLF, Science Park 104, 1098 XG Amsterdam, The Netherlands
‡Present address: Department of Chemistry and Applied Bioscience, ETH Zürich and Facoltà di Informatica, Istituto di Scienze Computazionali, Universita della Svizzera Italiana, Via Buffi 13 Lugano, CH-6900, Lugano, Switzerland.

1 Introduction

In this ESI we provide additional information. In particular, we give the anisotropy decay for both the SPC/E and TIP4P/2005 models for the fully hydrated and dehydrated systems, as well as protein-water HB lifetimes, reorientation time and structural parameters per area of the protein at different temperatures for wild type and mutant for the hydrated and dehydrated systems. In addition, we present the correlation between structure and dynamics in terms of the orientational order parameter q and the local structure index based parameter $S_{\rm lsi}$. for selected amino-acids at low temperature (270 K). Finally, we give the adsorption of wild type and mutant to the water-air interface of a slab geometry.

2 Methods

2.1 Local structure index

In addition to using the tetrahedral structural parameter S we also assess the water structure through the Local Structure Index (LSI). This function probes the gap between the first and second hydration shell[1], and quantifies the radial density fluctuations that occur within 3.8 Å around a reference water oxygen i. For each water oxygen i, one orders the n water oxygens within 3.8 Å of i according to their distance r as $r_1 < r_2 < \ldots < r_j < r_{j+1} < \ldots < r_n < 3.8$Å$< r_{n+1}$. The LSI is then given by

$$\mathrm{LSI} = \frac{1}{n}\sum_{j=1}^{n}(\Delta(j)-\bar{\Delta})^2, \qquad (1)$$

where $\Delta(j) = r_{j+1} - r_j$, and $\bar{\Delta}$ is the average of $\Delta(j)$. When water molecules form a tetrahedral structure locally, LSI increases, whereas for disordered water configurations, LSI decreases[1]. One can construct a distribution P(LSI) for water molecules i hydrating different amino-acids of the protein, and draw conclusions on the water translational structure. Shiratani et al.[1] identified two water populations, a structured (tetrahedral) and a disordered with LSI > 0.03 Å^2 and LSI < 0.03 Å^2, respectively. Following Ref.[1] we construct P(LSI) for every water i hydrating an amino-acid and use the integral of P(LSI) at LSI values higher or equal to a cutoff of 0.03 Å^2 to quantify the translational structure parameter $S_{\rm lsi}$.

2.2 Tetrahedral order parameter q

Another way to assess the water structure is via the tetrahedral order parameter q. This parameter, proposed by Errington and Debenedetti[2], is very sensitive to angular order and is calculated from the position of the four nearest oxygen atoms as follows:

$$\mathrm{q} = 1 - \frac{3}{8}\sum_{j=1}^{3}\sum_{k=j+1}^{4}\left(cos\psi_{jk}+\frac{1}{3}\right)^2, \qquad (2)$$

where angle ψ_{jk} connects the lines formed by the oxygen atom of water i, with the nearest oxygen atoms j and k. Note that in the case of hydration shell water, j,k can be any nearest hydrophilic group oxygen or nitrogen of the protein, or an oxygen of water.

2.3 Translational structure - water reorientation

To assess the correlation between structure and dynamics we constructed several 2D distributions. As mentioned above, each water i surrounding one amino acid for an mth interval of length ℓ, has a reorientation decay time $\tau_{i,m}$ associated with it. In the mth interval we also calculated the distribution $P(LSI_i)$ of waters i hydrating the same amino acid. From the normalized distribution $P(LSI_i)$ we obtain the structural parameter $S_{LSI,i,m}$ for each water i hydrating a particular amino acid, by integrating from 0.03 Å^2 onwards. We bin the pair $\tau_{i,m}$ and $S_{LSI,i,m}$ for each residue in a 2D histogram, in order to investigate possible correlation between water translational structuring and reorientation dynamics.

2.4 Orientational tetrahedral order - water reorientation

In the mth interval we also calculated the average q_i of waters i hydrating the same amino acid. We bin the pair $\tau_{i,m}$ and $q_{i,m}$ for each residue in a 2D histogram, in order to investigate possible correlation between water orientational tetrahedral structuring and reorientation dynamics.

3 Results

3.1 Anisotropy decay

From the MD simulations trajectories we calculated the anisotropy decay using Eq. 1 in the main text for all water molecules in the system and for the hydration shell water molecules only, for both wild type and mutant for different temperatures. The plots for the SPC/E and TIP4P/2005 model are shown in Figs. S1 and S2. As expected the anisotropy for all waters decays within a few ps for ambient conditions, but falls off much slower at lower temperatures. For the hydration water this effect is even more striking. In contrast to the bulk water, the hydration shell water experiences a heterogeneous environment, leading to an anisotropy decay that is non-exponential. Hydration water is significantly slower than bulk water.

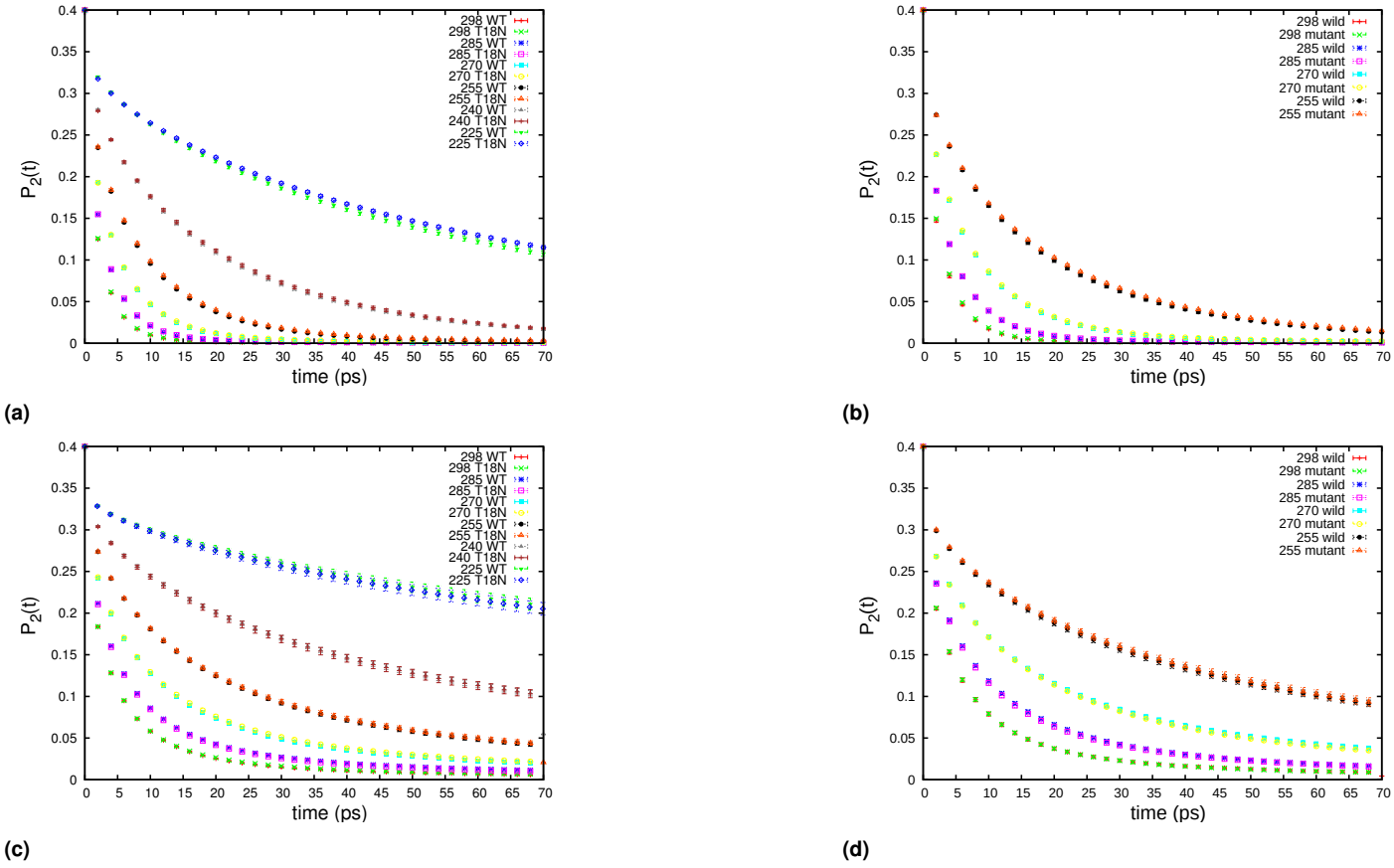

Figure S1 Anisotropy decay of all water of the fully hydrated a) SPCE systems and b) TIP4P/2005 systems. Anisotropy decay of hydration shell water of the fully hydrated c) SPCE systems and d) TIP4P/2005 systems.

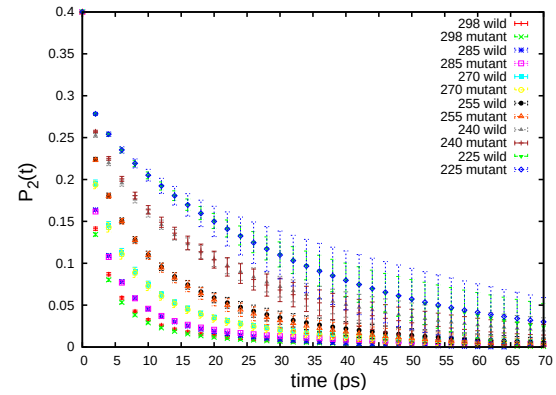

(a)

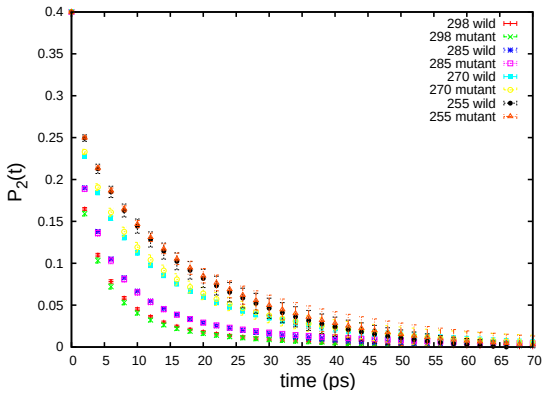

(b)

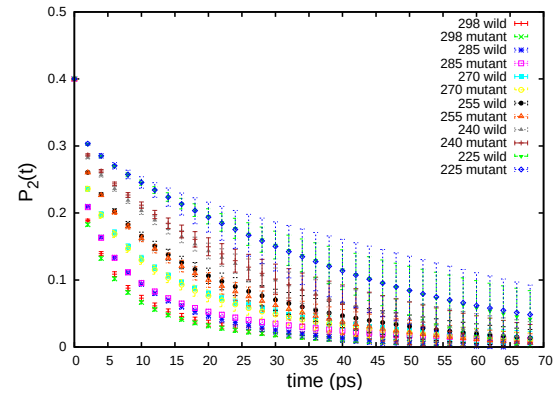

(c)

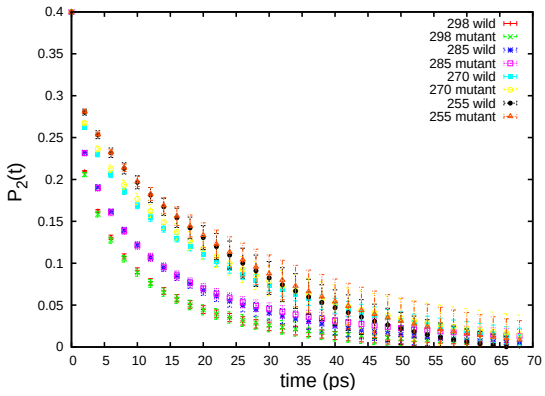

(d)

Figure S2 Anisotropy decay of all water of the dehydrated a) SPCE systems and b) TIP4P/2005 systems. Anisotropy decay of hydration shell water of the dehydrated c) SPCE systems and d) TIP4P/2005 systems.

3.2 Structure and dynamics as function of temperature

Figures S3-S8 show reorientation times, H-bond lifetimes and structural order parameter for water around different parts of the protein, as function of temperature for different systems, water models and hydration levels.

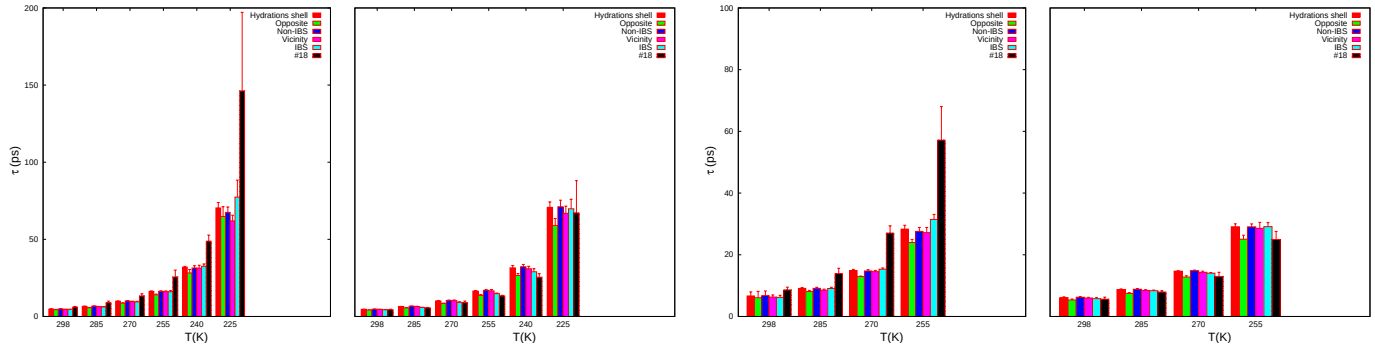

(a) SPCE **(b)** TIP4P/2005

Figure S3 Reorientation time of hydration water for all systems fully hydrated of study for the a) SPC/E and b) TIP4P/2005 water forcefield, wild (left) and mutant (right).

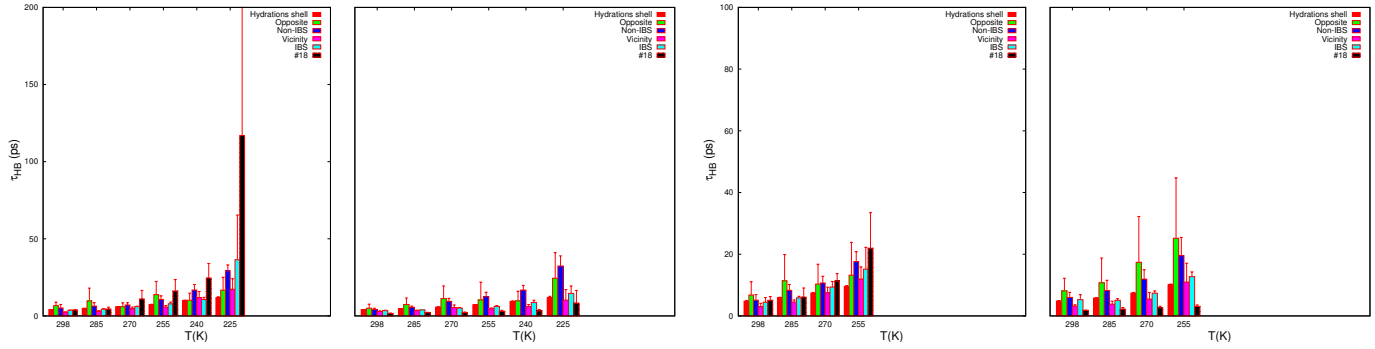

(a) SPCE **(b)** TIP4P/2005

Figure S4 Hydrogen bond lifetimes of hydration water for all fully hydrated systems of study for the a) SPC/E and b) TIP4P/2005 water forcefield, wild (left) and mutant (right).

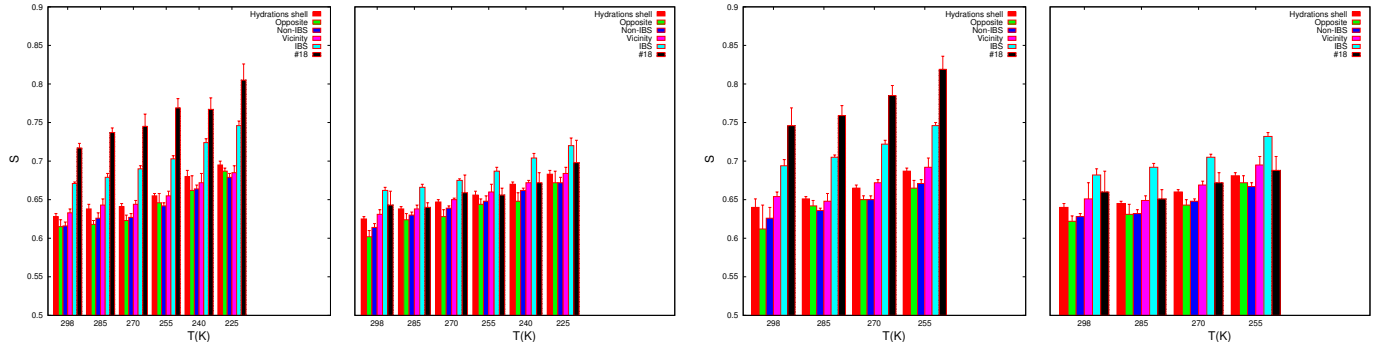

(a) SPCE **(b)** TIP4P/2005

Figure S5 Structural parameter S of hydration water for all fully hydrated systems of study for the a) SPC/E and b) TIP4P/2005 water forcefield, wild (left) and mutant (right).

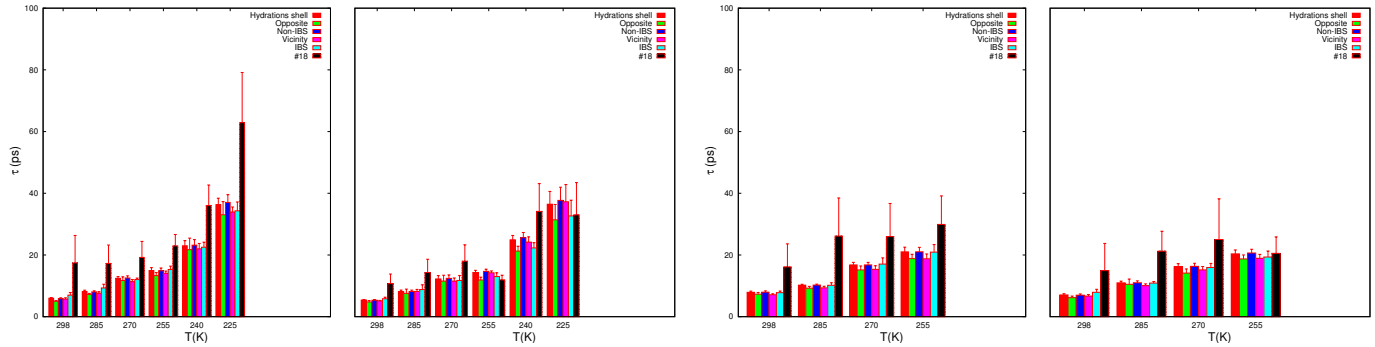

(a) SPCE **(b)** TIP4P/2005

Figure S6 Reorientation time of hydration water for all dehydrated systems of study for the a) SPC/E and b) TIP4P/2005 water forcefield, wild (left) and mutant (right).

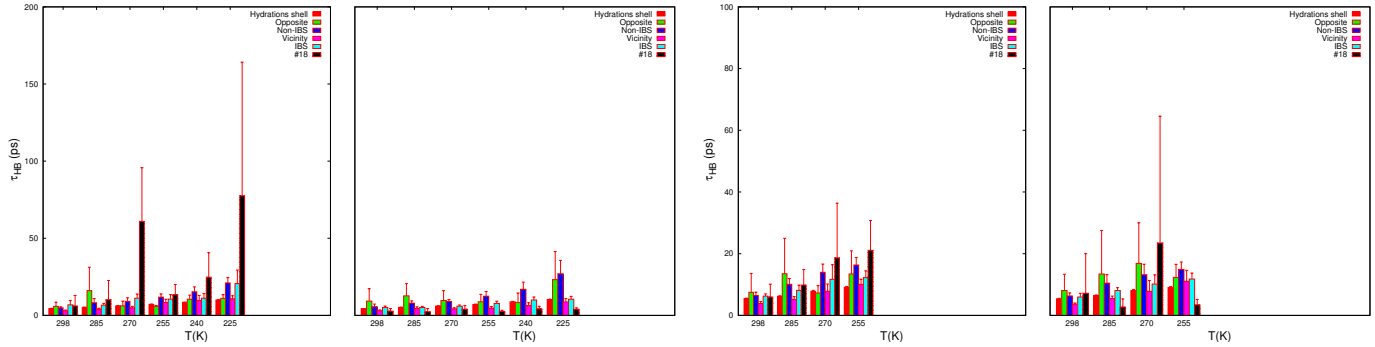

(a) SPCE **(b)** TIP4P/2005

Figure S7 Hydrogen bond lifetimes of hydration water for all dehydrated systems of study for the a) SPC/E and b) TIP4P/2005 water forcefield, wild (left) and mutant (right).

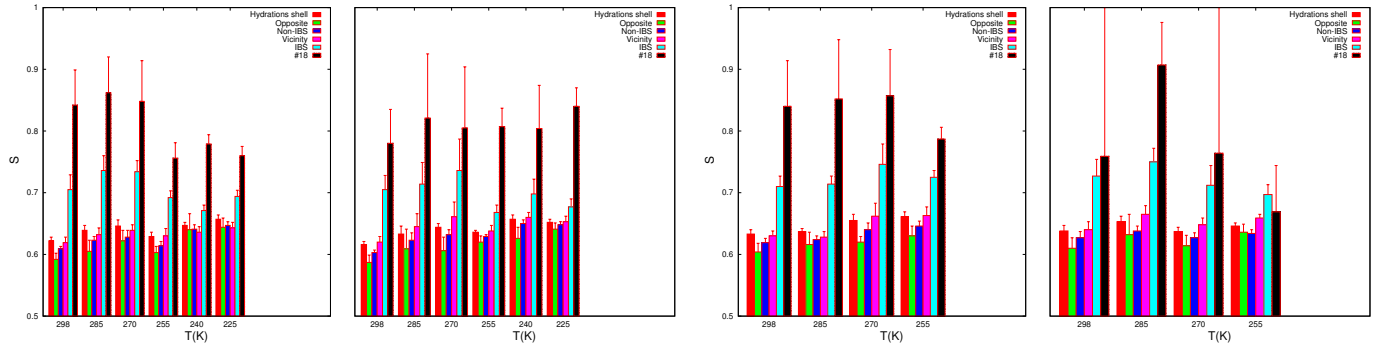

(a) SPCE **(b)** TIP4P/2005

Figure S8 Structural parameter S of hydration water for all dehydrated systems of study for the a) SPC/E and b) TIP4P/2005 water forcefield, wild (left) and mutant (right).

3.3 Hydration water structure

We plot the S_{lsi} for reference water molecules hydrating different parts of the protein (see Fig. S9). We observe a similar behaviour to tetrahedral structure order parameter. Water is translationally more structured at the protein compared to the bulk, and there is a subtle gradient of increasing translational structure from the opposite site towards the IBS. We find that upon mutation, there is a slight decrease of the translational structure locally to the mutation. This effect increases at lower temperatures (see Fig. S10)Finally, we plot the orientational order parameter q for water molecules hydrating different parts of the protein (see Fig. S11). We observe a similar gradient as for the other structural order parameters, where tetrahedral structure increases towards the IBS, albeit more subtle. Interestingly, bulk water shows the highest q value. This behaviour has been observed in simulation studies[3], and is understandable as q depends on water coordination, which decreases at the surface.

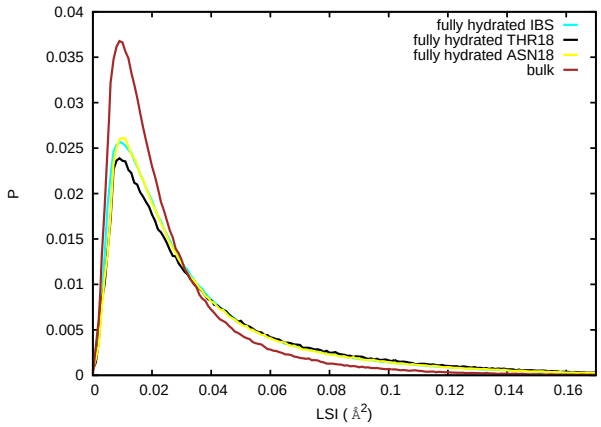

(a)

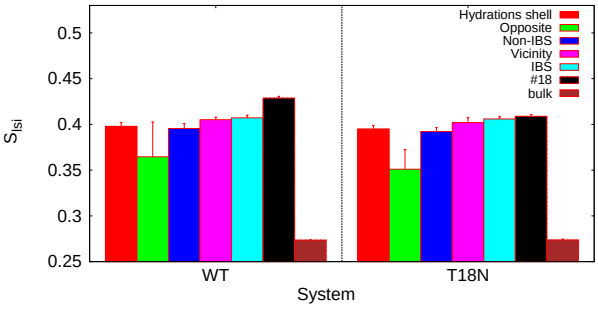

(b)

Figure S9 a) LSI distribution around reference water molecules solvating the wild fully hydrated system IBS (cyan), THR-18 of the wild fully hydrated system (black) , ASN-18 of the mutant fully hydrated system (yellow), of the bulk water (brown). b) Translational order parameter of water (S_{lSI}), for the different parts of the protein. All the above systems are in room temperature and for the SPC/E water systems. Color coding as in Fig 1. of the Main Text: IBS denoted by cyan, vicinity denoted by magenta, opposite denoted by green, THR-18 is denoted by black.

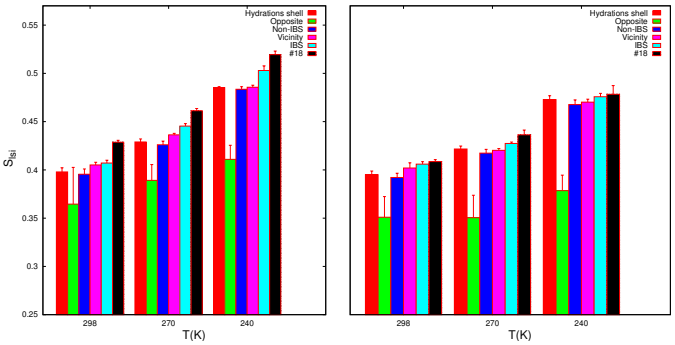

Figure S10 Structural parameter S_{lsi} of water at different parts of the protein for the fully hydrated system using SPC/E water forcefield, wild (left) and mutant (right) at 298K, 270K, and 240K.

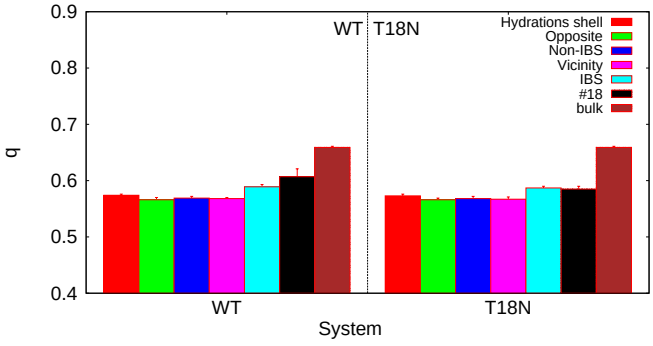

Figure S11 Orientational order parameter of water (q), for the different parts of the protein. All the above systems are at 270 K temperature and for the SPC/E water systems. Color coding as in Fig. 1 of the main text. See also Fig. S9

.

3.4 Correlation between structural paramter S and dynamics for low temperature

Figures S12 andS13 show the correlation between structure and dynamics for selected residues, for the wild type and mutant systems, at a temperature of 270 K. Fig. S15 and Fig. S16 show the h-bonded and non h-bonded disributions.

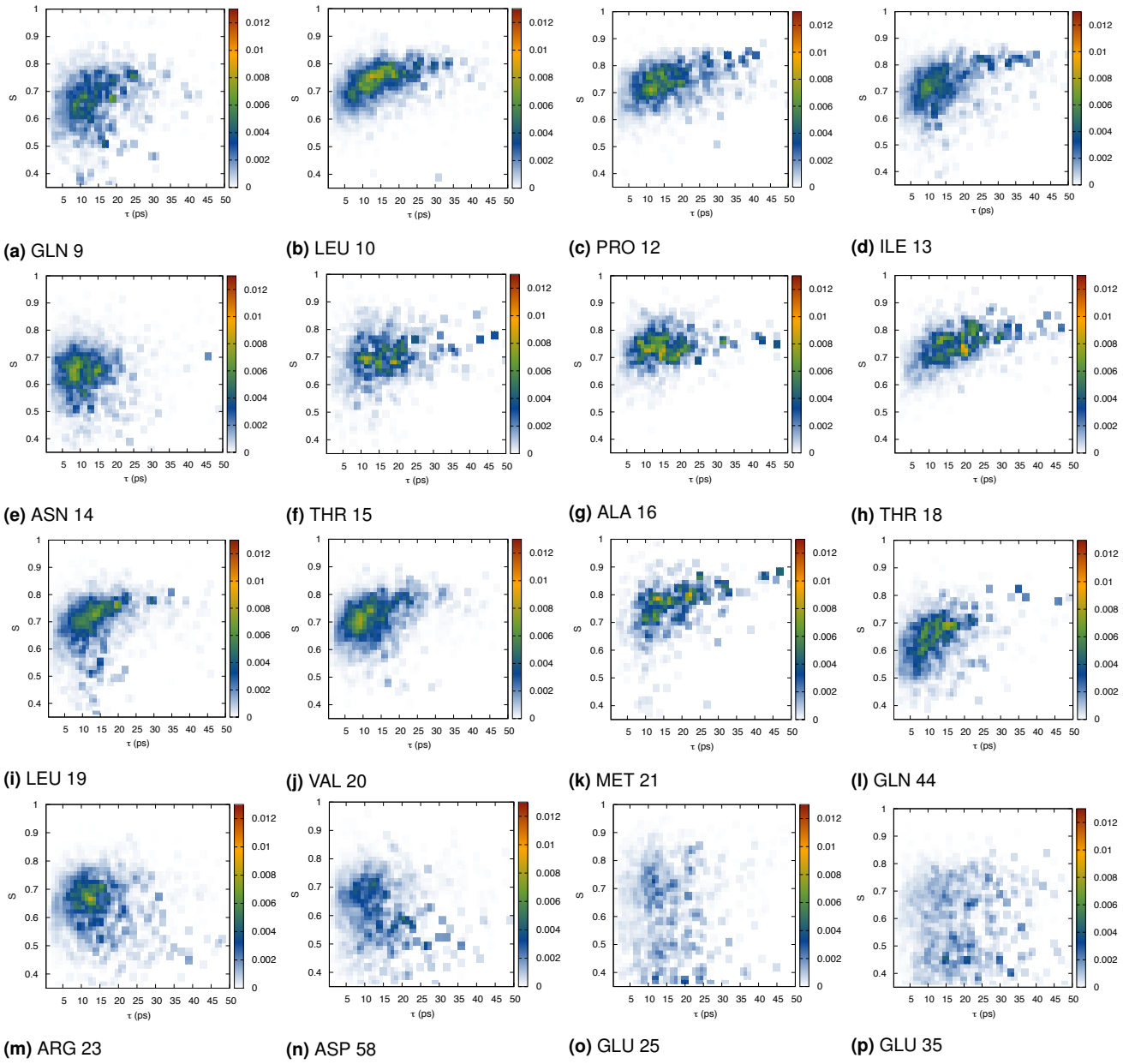

Figure S12 Reorientation decay time of water OH reorientation versus structure factor S for selected residues of WT at 270 K.

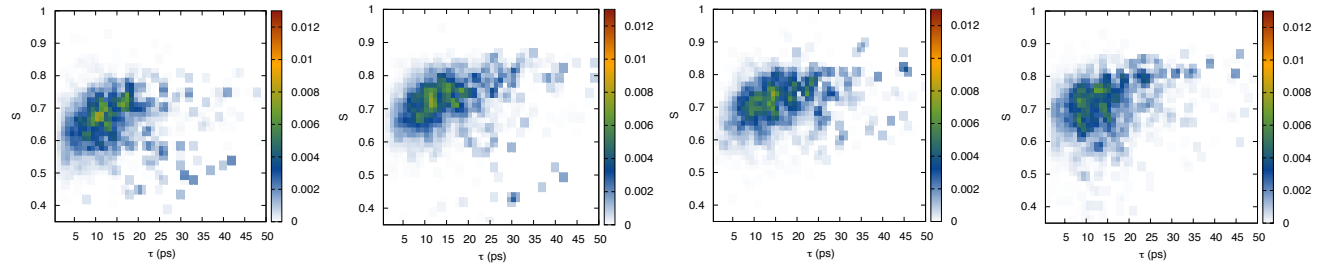

(a) GLN 9 **(b)** LEU 10 **(c)** PRO 12 **(d)** ILE 13

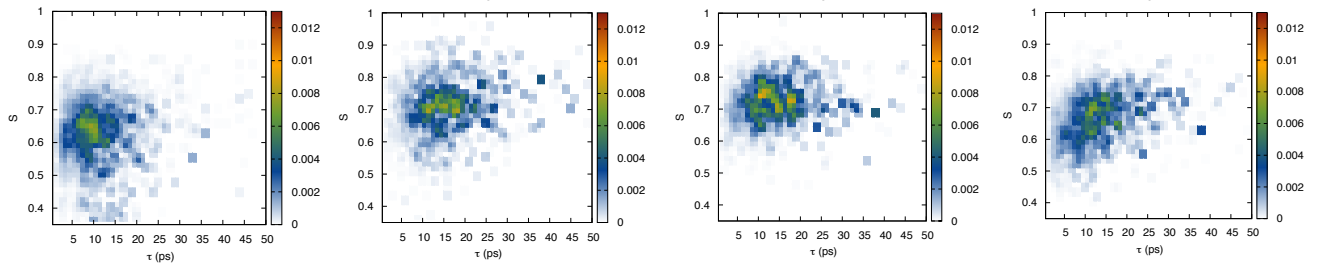

(e) ASN 14 **(f)** THR 15 **(g)** ALA 16 **(h)** ASN 18

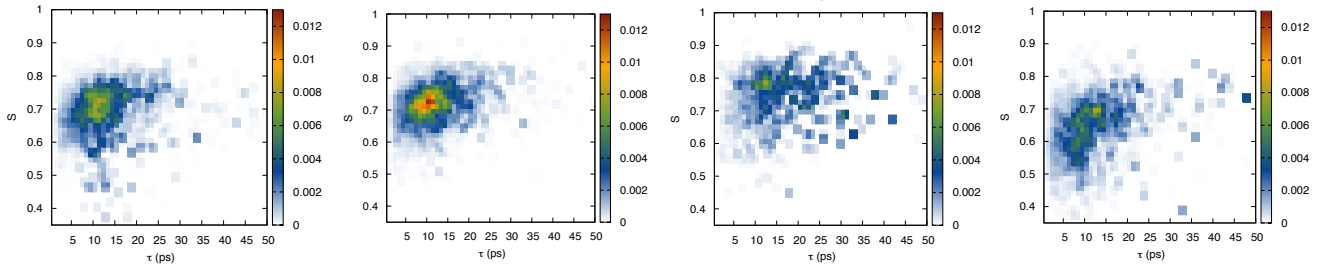

(i) LEU 19 **(j)** VAL 20 **(k)** MET 21 **(l)** GLN 44

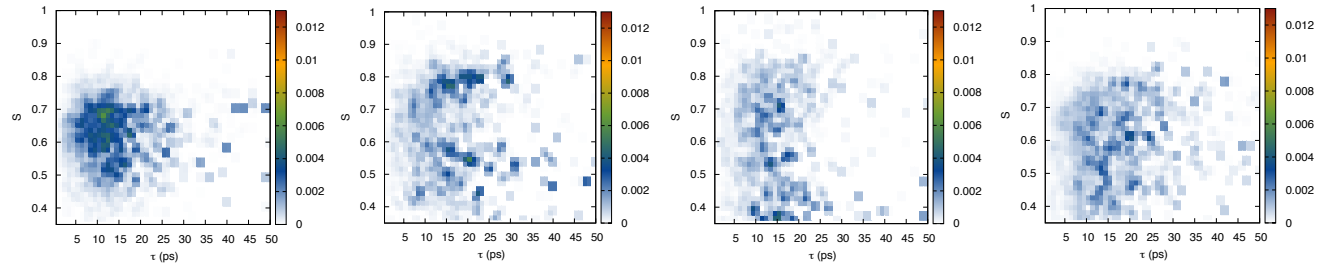

(m) ARG 23 **(n)** ASP 58 **(o)** GLU 25 **(p)** GLU 35

Figure S13 Reorientation decay time of water OH reorientation versus structure factor S for selected residues of T18N at 270 K.

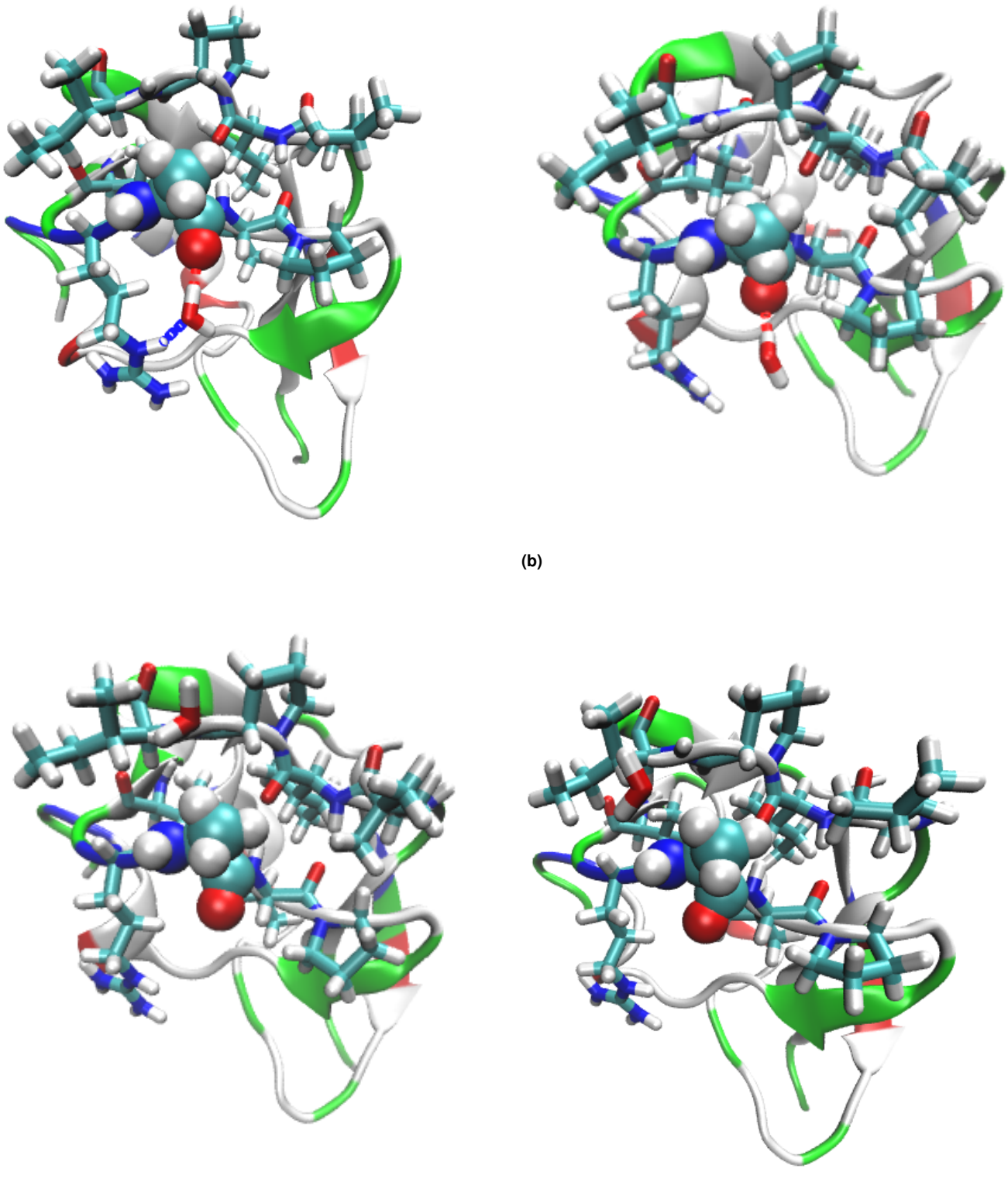

Figure S14 Configurations of the WT protein at 270 K. With VDW is depicted the residue ALA48, with licorice are the neighbouring residues within 0.44 nm, as well as a hydrating water belonging to the glass like negative S-τ population (a,b) and to the positive S-τ correlation population (c,d).

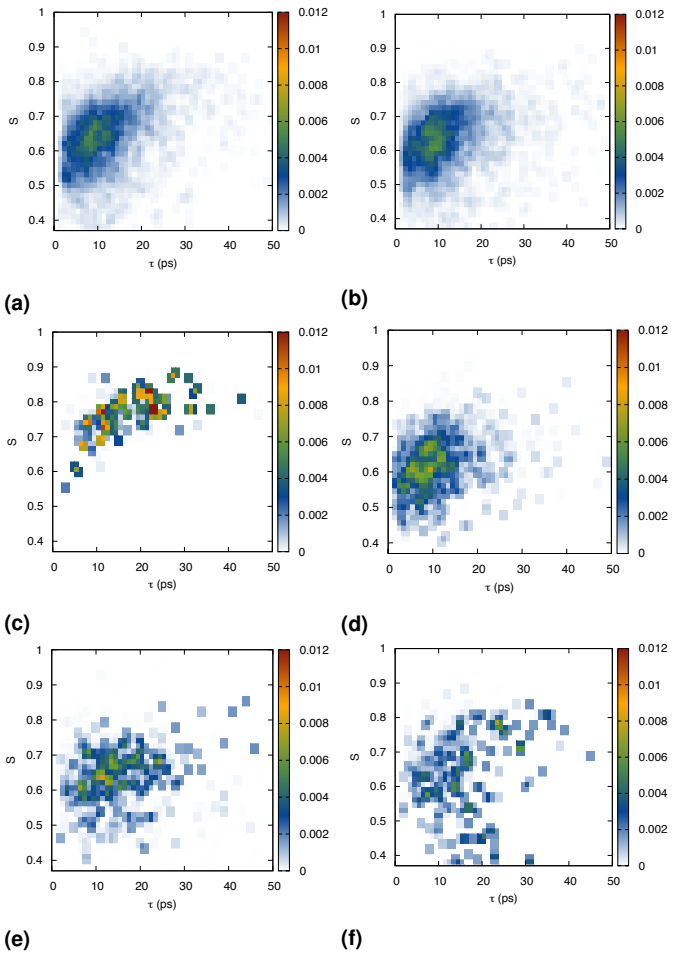

Figure S15 Structural parameter S as a function of water reorientation decay time for selected residues, and for their H-bonded population to the protein, of a) IBS (WT), b) IBS (T18N), c) THR-18 (WT), d) ASN-18 (T18N), e) ARG-39 (WT/vicinity), f) ALA-48 (WT/vicinity) at 270 K.

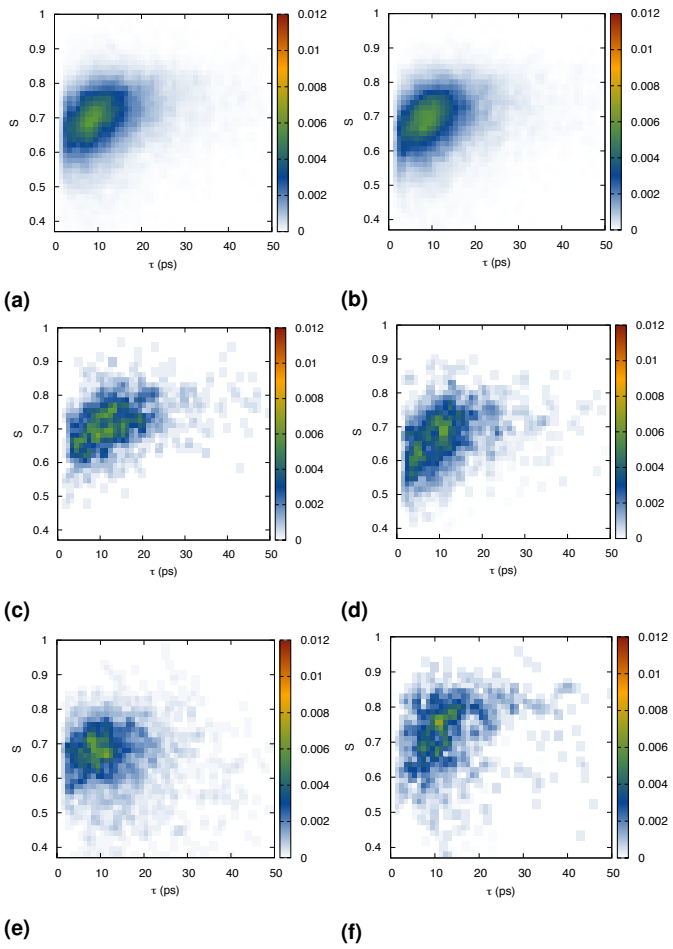

Figure S16 Structural parameter S as a function of water reorientation decay time for selected residues, and for their not H-bonded population to the protein, of a) IBS (WT), b) IBS (T18N), c) THR-18 (WT), d) ASN-18 (T18N), e) ARG-39 (WT/vicinity), f) ALA-48 (WT/vicinity) at 270 K.

3.5 Translational structure - reorientation time correlation.

In addition, we investigate the correlation between the water reorientation dynamics and translational structure by histogramming the hydrating waters as function of their S_{lsi} and τ_i, where we weight each entry with a factor ℓ (see Methodology section). Figures S17 and S18 show the 2D histograms of S_{lsi} and τ_i of the IBS and of selected amino acids, respectively, at 298 K and 270 K for the wild type and mutant SPC/E system.

Similar to the tetrahedral structure-water reorientation at room temperature the IBS of the wild type shows clearly a positive correlation between translational structure S_{lsi} and water reorientation time (τ) in Fig. S17a,b. While this correlation is not perfect, clearly, water that is more translationally ordered is likely to exhibit a longer reorientation time. The S_{lsi} of respective IBS's S_{lsi} hardly changes upon mutation. For residue 18, S_{lsi} indicates a slight decrease in the translational structure of ASN-18 compared to THR-18 (see Fig. S10 and Fig. S17c,d). Similar to the tetrahedral structural analysis, the charged residue ARG-39 shows on average less translational structure compared to more hydrophobic THR-18. As shown in (Fig. S17a,b,c,d) the S_{lsi}-τ correlation of the WT IBS vs T18N IBS and THR-18 vs ASN-18 are similar.

Upon cooling the system to 270 K, the difference between the S_{lsi} of WT IBS and T18N IBS is again negligible, whereas that of THR-18 and ASN-18 show a slight decreace upon mutation. The WT charged ARG-39 has a lower translation structure than the IBS. The S_{lsi}-τ curves, while showing similar trends as the tetrahedral structure-reorientation correlation plots (Figures 6 and 7 of the main text, vs. Fig. S17, and Fig. S18), are nonlinear and often saturate around $S_{lsi} = 0.5$. Most hydrophobic IBS amino-acids have a positive S_{lsi} -τ correlation (see Fig. S18, Fig. S19, Fig. S20). The charged amino-acid ARG-39 (see Fig. S18e) shows hardly any correlation, in contrast to the negative correlation in Figure 6e and Figure 7e of the main text. Also, residue ALA-48, which in the tetrahedral analysis showed both negative and positive correlation, now has a positive correlation only.

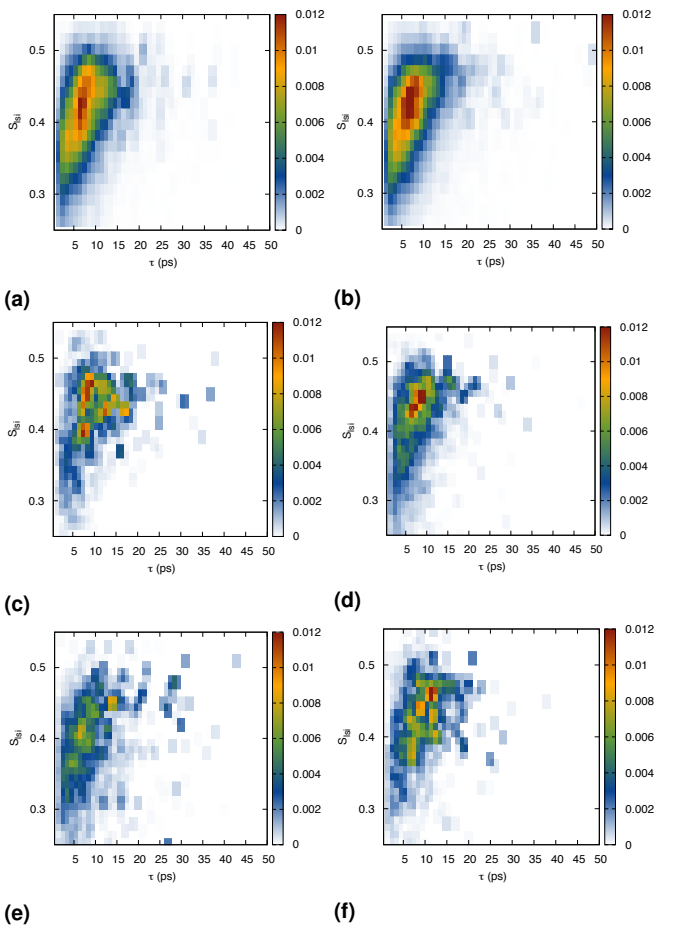

Figure S17 Structural parameter S_{lsi} as a function of water reorientation decay time for selected residues of a) IBS (WT), b) IBS (T18N), c) THR-18 (WT), d) ASN-18 (T18N), e) ARG-39 (WT/vicinity), f) ALA-48 (WT/vicinity) at 298 K.

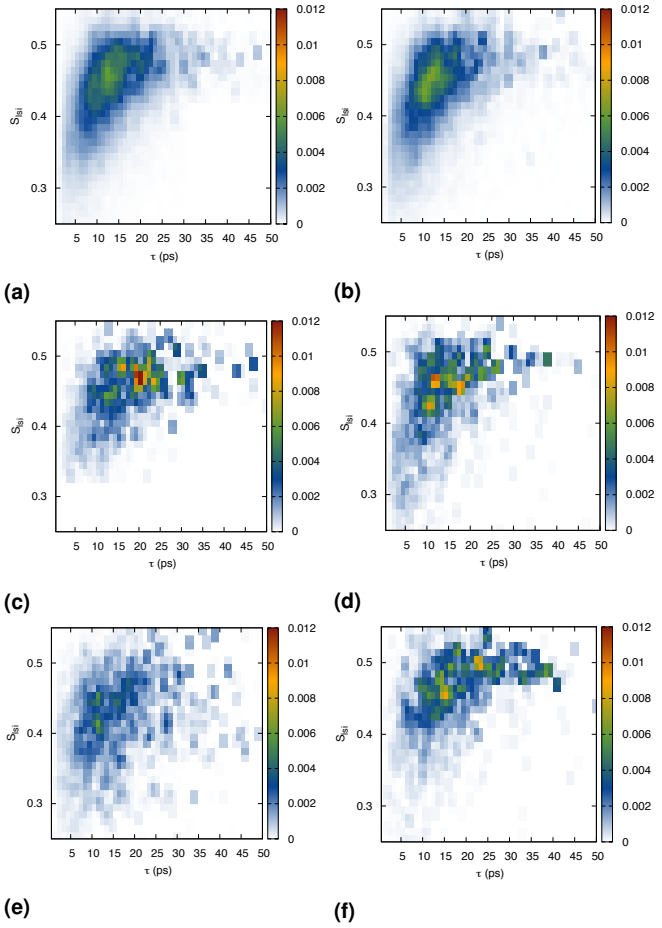

Figure S18 Structural parameter S_{lsi} as a function of water reorientation decay time for selected residues of a) IBS (WT), b) IBS (T18N), c) THR-18 (WT), d) ASN-18 (T18N), e) ARG-39 (WT/vicinity), f) ALA-48 (WT/vicinity) at 270 K.

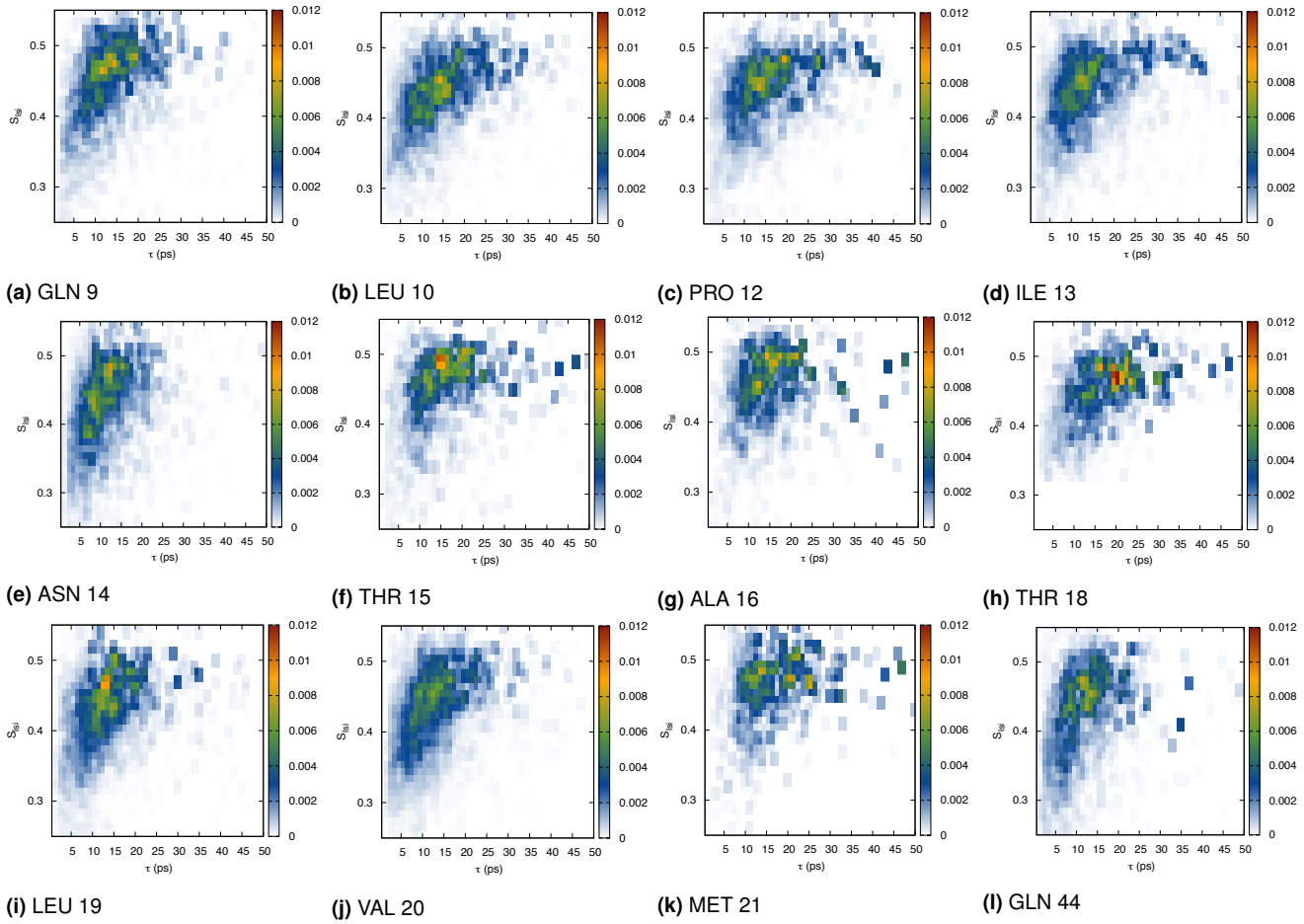

Figure S19 Reorientation decay time of water OH reorientation versus structure factor S_{lsi} for selected residues of WT at 270 K.

Overall, the translational structure -reorientation time correlation is not as strong and clear cut as for the tetrahedral order parameter, and S_{lsi} does not discriminate very well between the different residues. This is possibly because the translational structure order parameter S_{lsi} is less sensitive to the water OH orientation dynamics compared to the OOH tetrahedral structure order parameter, as it probes fluctuations far away from the reference water that is used for the reorientation calculations, i.e. between the first and second shell. While the analyses of the two structural order parameter are not in disagreement, the tetrahedral structural order parameter S is the more sensitive one.

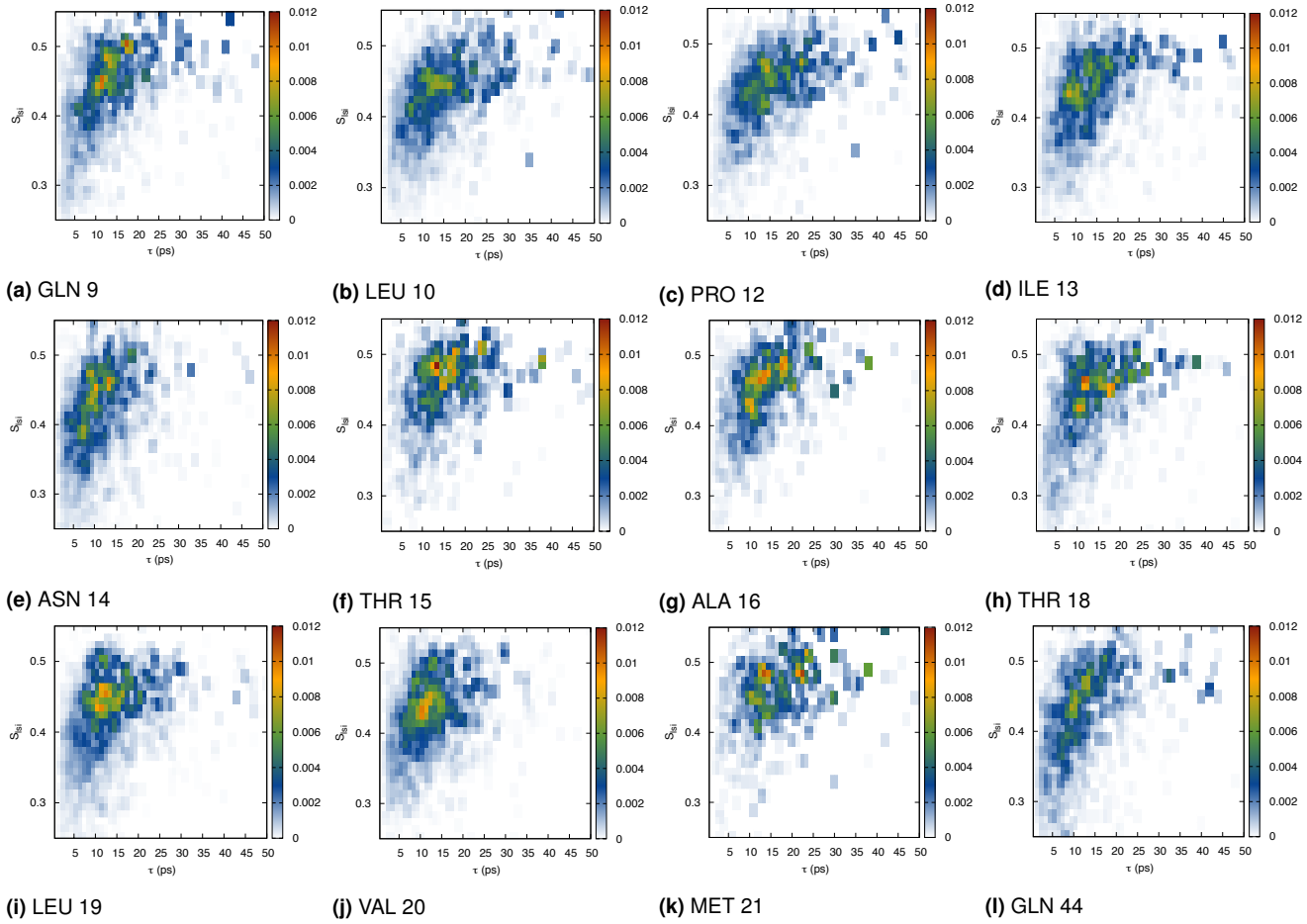

(a) GLN 9 **(b)** LEU 10 **(c)** PRO 12 **(d)** ILE 13

(e) ASN 14 **(f)** THR 15 **(g)** ALA 16 **(h)** THR 18

(i) LEU 19 **(j)** VAL 20 **(k)** MET 21 **(l)** GLN 44

Figure S20 Reorientation decay time of water OH reorientation versus structure factor S_{lsi} for selected residues of T18N at 270 K.

3.6 Orientational tetrahedral structure - reorientation time correlation.

To validate our findings we plot the overall orientational tetrahedral order parameter q, w.r.t. to the reorientation dynamic correlation (see Fig. S21.). Moreover, to gain insight on the effect of hydrogen bonding or non hydrogen bonding on the $(q-\tau)$ fingerprint, we split the overall distribution to the ones corresponding to the fraction of time the water i was H-bonded to the protein or not (see Fig. S22, and Fig. S23). We find that although the overall distributions show a more convoluted picture of positive and negative $q-\tau$ correlation, the IBS and the THR-18 have a more pronounced positive correlation population (see Fig. S21a,c), and that charged amino acids, such as ARG-39, have a less positive correlation (Fig. S21d). Interestingly, when splitting the distribution, we find that the negative correlation population (low q,high τ) are due to the H-bonded population (Fig. S22, and the positive correlation of q,τ (high q, high τ) is mostly due to the non H-bonded to the protein water population (Fig. S23). The slight negative correlation in (Fig. S23) is attributed to the fact that a water that is non H-bonded to the protein can still be influenced by the protein. Strikingly, the q values is now lower for the h-bonded population in Fig. S22 compared to the non h-bonded values in Fig. S23). This is explained by the fact that q is more sensitive to the effect of the under-coordination caused by the surface (since it depends on 4 correctly placed O or N) than S (which depends on a pair angle). This means that h-bonded waters such as for THR-18 (WT) show actually a lower q than the non-bonded water. This is also corroborated by the fact that q is highest in bulk water, and decreases towards the surface. Nevertheless, it is clear from the difference between Fig. S22c and Fig. S22e, that the q values for THR-18 are higher than that for vicinity residues such as ARG-39, in agreement with Fig. S11, thus corroborating our findings. However, just as the case with the translation structural parameter S_{lsi}, while the results are certainly not disagreeing q cannot discriminate between the nature of the IBS and vicinity residues as the tetrahedral structural parameter S can. Hence, in the main text we emphasize this parameter.

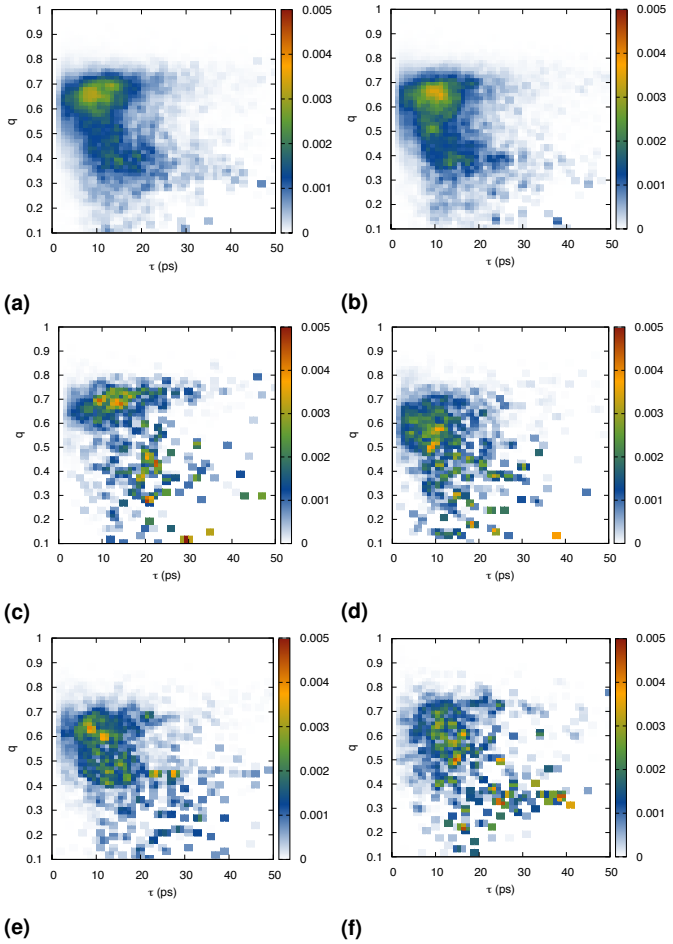

Figure S21 Structural parameter q as a function of water reorientation decay time τ for selected residues of a) IBS (WT), b) IBS (T18N), c) THR-18 (WT), d) ASN-18 (T18N), e) ARG-39 (WT/vicinity), f) ALA-48 (WT/vicinity) at 270 K.

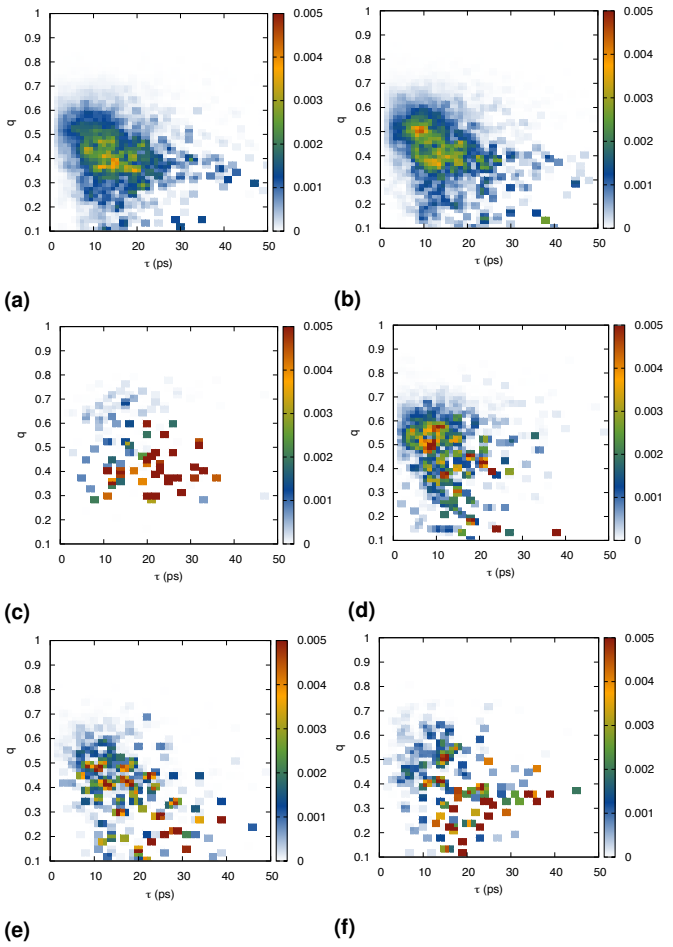

Figure S22 Structural parameter q as a function of water reorientation decay time τ for selected residues, and for their H-bonded population to the protein, of a) IBS (WT), b) IBS (T18N), c) THR-18 (WT), d) ASN-18 (T18N), e) ARG-39 (WT/vicinity), f) ALA-48 (WT/vicinity) at 270 K.

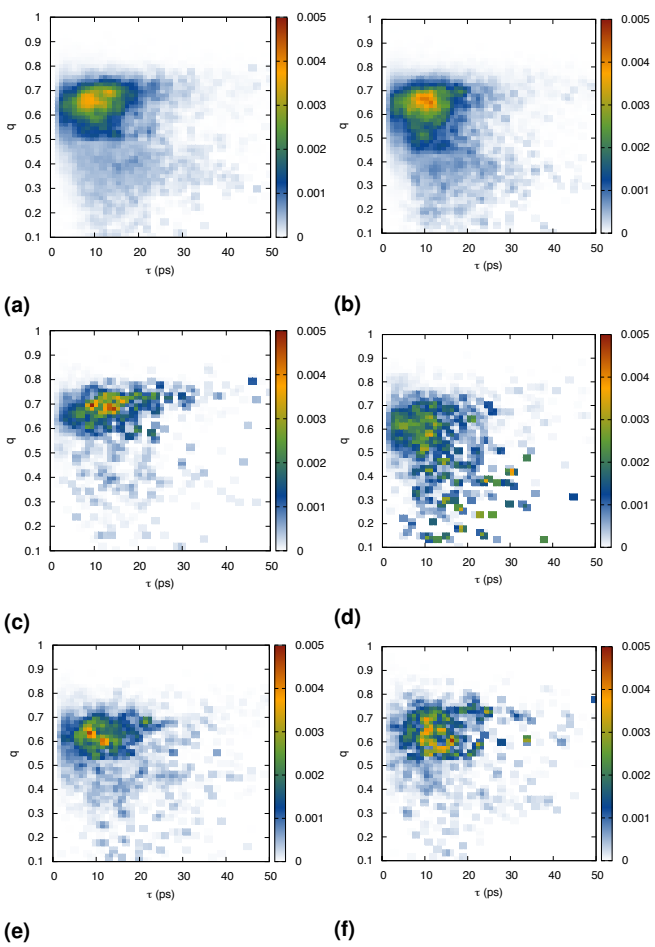

Figure S23 Structural parameter q as a function of water reorientation decay time for selected residues, and for their not H-bonded population to the protein, of a) IBS (WT), b) IBS (T18N), c) THR-18 (WT), d) ASN-18 (T18N), e) ARG-39 (WT/vicinity), f) ALA-48 (WT/vicinity) at 270 K.

3.7 Adsorption to water-air interface

Fig. S24 shows the time evolution of the z-coordinate of residue 18 along an MD trajectory. Fig. S25 shows the distribution for different cutoffs for identifying hydration.

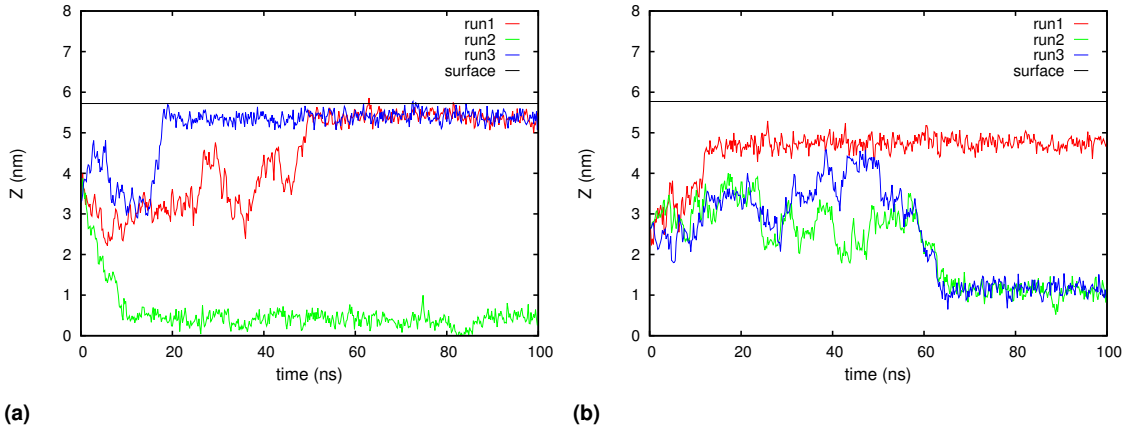

Figure S24 Absolute z coordinate of the center of mass of a) THR-18 at WT slab system and b) ASN-18 at T18N slab systems respectively. The water slab lies between Z=0 and the black line at the position 5.82 nm.

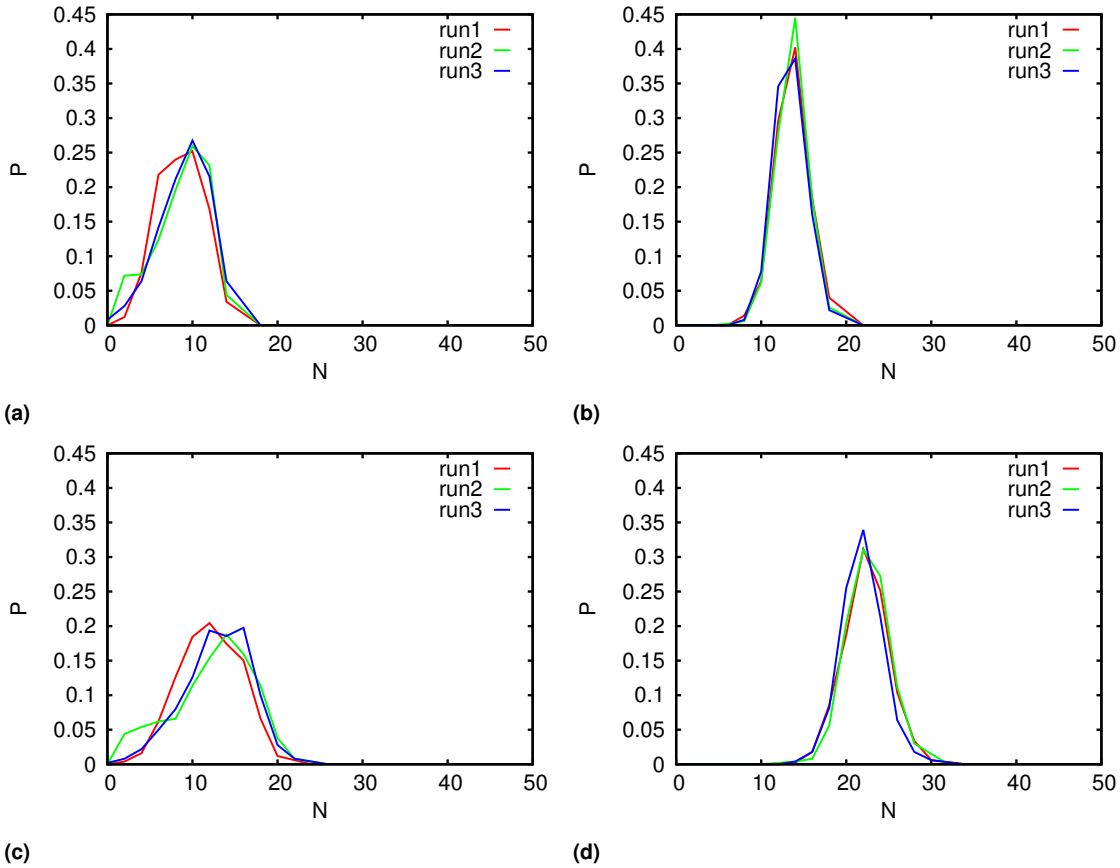

Figure S25 Distribution of water molecules within 0.45 nm of a) THR-18 and b) ASN-18 and within 0.55 nm of c) THR-18 and d) ASN-18. The left column corresponds to the WT slab system and the right to the T18N slab system.

3.8 Protein stability

In this subsection, we assess the stability of the WT and T18N fully hydrated proteins at 298 K and 270 K. We present the RMSD of the protein's CA atoms, compared to the PDB crystal structures of the wild type (1HG7) and mutant (1JAB) at 298 K and 270 K respectively.As shown in Fig. S26a the RMSD value and fluctuations of the WT and T18N protein compared to each respective PDB's is within the experimental resolution of these PDBs (0.15 nm for 1HG7 and 0.165 for the 1JAB). Moreover, the solvent accessible surface of the protein in the above-mentioned systems is the same within fluctuations as shown in Fig. S26b. Hence, the proteins are stable and do not exhibit large conformational changes in the 100 ns runs. We therefore assume the proteins to be equilibrated.

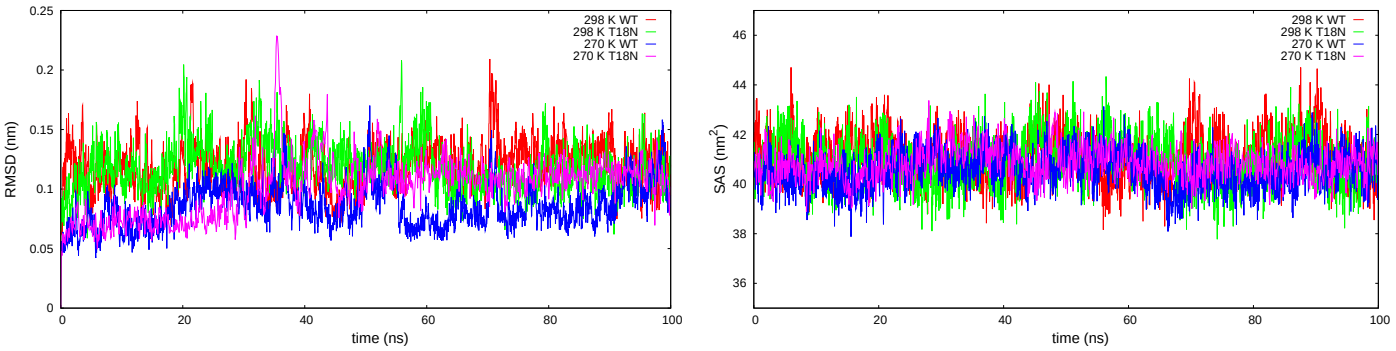

(a) **(b)**

Figure S26 a) RMSD of the protein's CA atoms, compared to the PDB crystal structures of the wild type (1HG7) and mutant (1JAB) at 298 K and 270 K respectively. b) Solvent accessible surface of the protein atoms of the WT and T18N at 298 K and 270 K .

References

[1] E. Shiratani and M. Sasai, *J. Chem. Phys.*, 1996, **104**, 7671–7680.

[2] J. Errington and P. Debenedetti, *Nature*, 2001, **409**, 318–321.

[3] S. S. Mallajosyula, K. Vanommeslaeghe and A. D. Mackerell, *J. Phys. Chem. B*, 2014, **118**, 11696–11706.